How to cite: *Angew. Chem. Int. Ed.* **2021**, *60*, 23695 – 23704
International Edition: doi.org/10.1002/anie.202104794
German Edition: doi.org/10.1002/ange.202104794

Photoswitches

Pyrrole Hemithioindigo Antimitotics with Near-Quantitative Bidirectional Photoswitching that Photocontrol Cellular Microtubule Dynamics with Single-Cell Precision**

*Alexander Sailer, Joyce C. M. Meiring, Constanze Heise, Linda N. Pettersson, Anna Akhmanova, Julia Thorn-Seshold, and Oliver Thorn-Seshold**

Abstract: *We report the first cellular application of the emerging near-quantitative photoswitch pyrrole hemithioindigo, by rationally designing photopharmaceutical* ***PHTub*** *inhibitors of the cytoskeletal protein tubulin.* ***PHTub****s allow simultaneous visible-light imaging and photoswitching in live cells, delivering cell-precise photomodulation of microtubule dynamics, and photocontrol over cell cycle progression and cell death. This is the first acute use of a hemithioindigo photopharmaceutical for high-spatiotemporal-resolution biological control in live cells. It additionally demonstrates the utility of near-quantitative photoswitches, by enabling a dark-active design to overcome residual background activity during cellular photopatterning. This work opens up new horizons for high-precision microtubule research using* ***PHTub****s and shows the cellular applicability of pyrrole hemithioindigo as a valuable scaffold for photocontrol of a range of other biological targets.*

Introduction

Optically targeted approaches to manipulate biological systems have revolutionised diverse research fields, by enabling the non-invasive patterning of protein activity with resolution on the spatial and temporal scales inherent to cellular functions. The high-precision studies that optical approaches allow have particular promise for systems whose spatiotemporal regulation is key to their functions: such as action potential firing in neuroscience, or cytoskeleton structure and dynamics in cell biology.[1–3] The major optical approaches are optogenetics,[4] photouncaging,[5] and photopharmacology.[6] Photopharmacology offers both distinct performance and a unique application space. Unlike photouncaging, photopharmaceuticals can be modulated reversibly, to avoid a build-up of background bioactivity that could compromise biological readout; their photoresponse is near-instantaneous and does not generate toxic uncaging by-products; and their photoresponse wavelengths are often more biologically compatible and more tunable than those of caging groups.[7,8] Unlike optogenetics, photopharmaceuticals do not need genetic engineering, so they transition easily between biological models; and they can target proteins which do not allow functional photocontrol by fusion constructs, such as the cytoskeletal scaffolds tubulin and actin.[3,8,9] Since the spatiotemporally precise orchestration of cytoskeleton structure and dynamics is critically important to hundreds of biological processes, cytoskeleton photopharmaceuticals have emerged as a valuable goal of research in recent years.[10,11] They hold promise for basic research into anisotropic processes, for example, in intracellular transport, mechanostasis and cell motility, as well as for applied research on, for example, anti-invasive strategies in cancer therapy.[10,12,13]

The development of photopharmaceuticals has however been held back by the limited space of photoswitch scaffolds shown to permit bioactivity photoswitching in cells, and by their drawbacks. An "ideal" photoswitch scaffold would permit near-complete, bidirectional photoisomerisations in situ in live cells under practical conditions, to allow efficient and precise photopatterning of its photoisomers. An ideal photopharmaceutical would further decorate this scaffold to create a ligand with near-zero bioactivity as one isomer, and potent bioactivity as the other isomer. The vast majority of cellularly applicable photopharmaceuticals rely on azobenzene scaffolds, with diarylethenes, fulgides and hemithioindigos as minor players (Figure 1a); yet these scaffolds are far from ideal. Here we expand the space of cellular photoswitch scaffolds, tackling two performance problems that azobenzenes in particular fail to address. In doing so we provide both a useful new reagent for photocontrol of the microtubule (MT) cytoskeleton, and general advances for practical photopharmacology.

The first disadvantage of current photoswitches that we focus on, is that, typically, they cannot be quantitatively bidirectionally photoisomerised with biologically compatible

[*] A. Sailer, C. Heise, L. N. Pettersson, Dr. J. Thorn-Seshold, Dr. O. Thorn-Seshold
Department of Pharmacy
Ludwig-Maximilians University of Munich
Butenandtstrasse 7, 81377 Munich (Germany)
E-mail: oliver.thorn-seshold@cup.lmu.de
Dr. J. C. M. Meiring, Prof. Dr. A. Akhmanova
Department of Biology, Utrecht University
Padualaan 8, 3584 Utrecht (The Netherlands)

[**] A previous version of this manuscript has been deposited on a preprint server (https://doi.org/10.26434/chemrxiv.14130107.v1).
Supporting information and the ORCID identification number(s) for the author(s) of this article can be found under: https://doi.org/10.1002/anie.202104794.

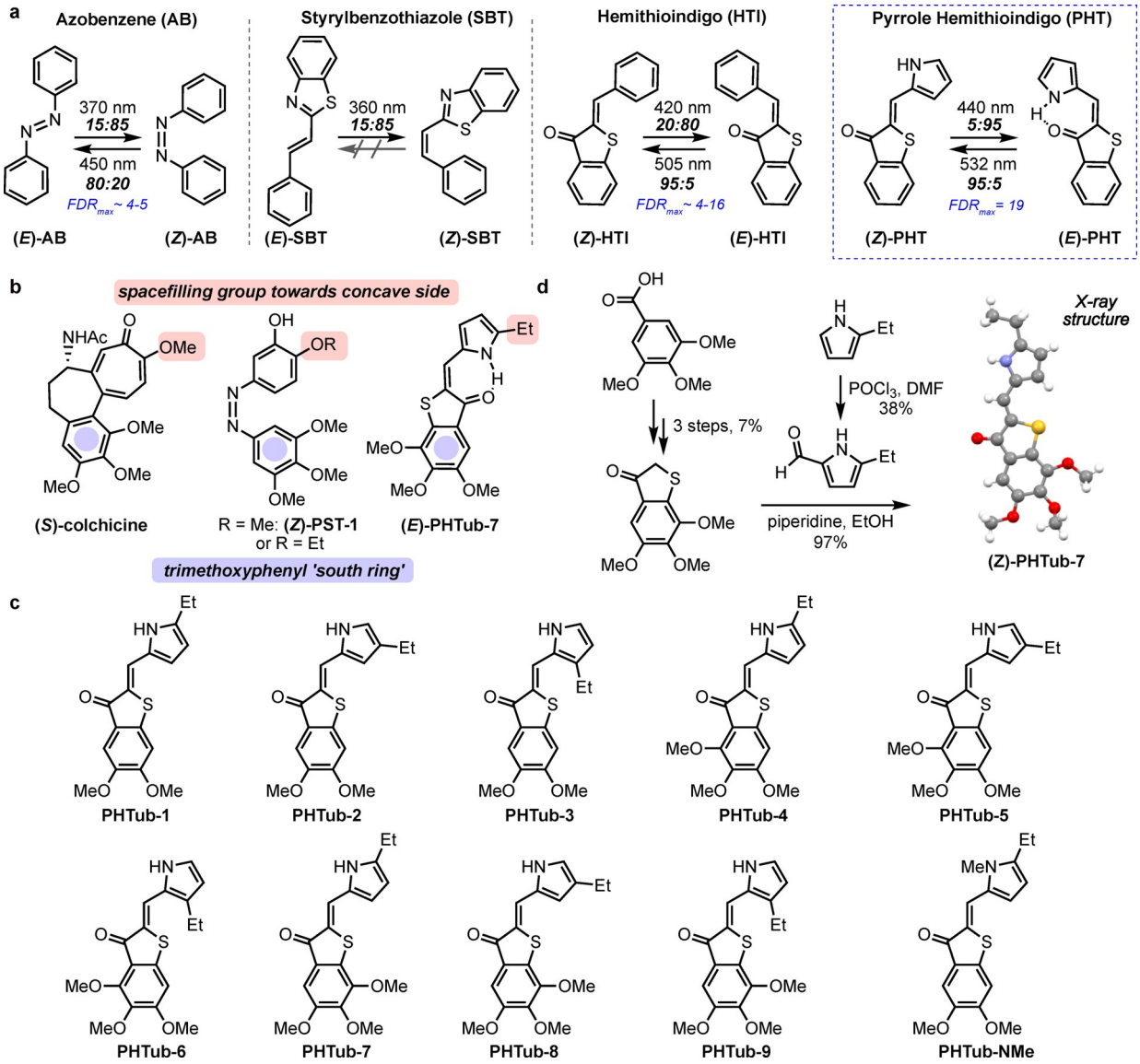

Figure 1. Design and synthesis of **PHTub**s: a) Photoswitchable scaffolds azobenzene, styrylbenzothiazole, hemithioindigo, and pyrrole hemithioindigo, with typical best photostationary state isomer ratios achieved under photoswitching in the biologically compatible wavelength range, and corresponding FDR_{max} values. b) **PHTub**s designed by derivatising PHT towards the pharmacophore requirements of the colchicine binding site on tubulin. c) Structures of **PHTub**s synthesised and tested in this study. d) Summary synthesis of representative reagent, **PHTub-7**, by piperidine-catalysed aldol condensation of the corresponding thioindoxyl and pyrrole carboxaldehyde; **PHTub-7** is depicted using its X-ray crystal structure (*Z* isomer).

wavelengths, which limits their power to photopattern biological activity. Using azobenzene as the most important example, its largest typical change of photostationary state (PSS) composition is around 4–5-fold (between ca. 15:85 *trans*:*cis* under 370 nm and ca. 80:20 *trans*:*cis* under 450 nm, though new polysubstituted or heteroaromatic azobenzenes can perform better).[1,14–16] Thus, even if only one of an azobenzene's two isomers is biologically active, photoswitching with cell-compatible wavelengths (>360 nm) can, in a best-case scenario, achieve just 4–5-fold photocontrol over the concentration patterning of the bioactive species. We define this useful quantity of the photoswitch scaffold as its maximum functional dynamic range, FDR_{max} [Eq. (1)], where

$$FDR_{max} = \frac{\phi_F}{\phi_B} \quad (1)$$

ϕ_F is the fraction of the biologically more active isomer after the most complete "forwards" photoisomerisation (PSS with the highest content of this isomer), and ϕ_B is the remaining fraction of that isomer after the most complete back-isomerisation. Note however, that typical photopharmaceuticals have substantial residual bioactivity in the less active isomer: so their actual functional dynamic range of bioactivity (FDR) cannot approach the FDR_{max}, which only reflects scaffold isomerisation (Figure 1 a).

The second disadvantage we focus on, is that the fixed-wavelength lasers available to biologists cannot deliver these "best-case" isomerisations, since typical confocal microscopes

only have a subset of the 405, 442, 488, 514, 561, and 647 nm laser lines.

These disadvantages can combine to ruin the performance of even biologically well-designed photopharmaceuticals. For example, the MT-inhibiting azobenzene **PST-1** (Figure 1b),[3,17–19] designed towards an exceptional 10000-fold difference of tubulin-binding affinity between the photoisomers,[20] has a FDR_{max} of just 9-fold with "best-case" photoisomerisations (380/525 nm). This is still comparatively high for azobenzenes; but with biologically available laser lines, the practical FDR that can be reached is just 3-fold (405/514 nm): a sharp loss of potential for an otherwise excellent photopharmaceutical.[3]

To create practical MT cytoskeleton photopharmaceuticals, we therefore focussed on photoswitch scaffolds with high FDR_{max} that also match to biologically accessible visible-light lasers. Previous explorations of C=C-based photoswitches (405 nm-switchable styrylbenzothiazole[21] as well as visible-light-switchable hemithioindigos;[22–26] Figure 1a) have highlighted their robustness to glutathione (GSH)[27] as well as their tolerance of tautomerisable polar functional groups (e.g. *para*-hydroxy groups) that are important for ligand–target interactions. These features make C=C-based photoswitches attractive for further research, particularly compared to azobenzenes, which are known to suffer GSH lability, and where tautomerisable functional groups counteract their photoisomer patterning.[28,29]

Newhouse and Zweig recently developed the C=C-based photoswitch pyrrole hemithioindigo (PHT, Figure 1a), which has an outstanding FDR_{max} of ca. 40 in organic media, due to band separation between the groundstate *Z* and metastable *E* isomers, driven by the *E* isomer's intramolecular pyrrole NH···O=C carbonyl hydrogen bond.[27,30] While the photostability and GSH resistance of PHT encourage biological use, their report described insolubility and poor/zero photoswitching in increasingly aqueous media.[27] However, we previously observed that polymethoxylated derivatives of otherwise low-solubility scaffolds can be photoswitched repeatedly in situ in cells, to photopattern bioactivity with performance recalling that seen in apolar media.[31] We attributed this to cellular sequestration of the hydrophobic photoswitches primarily in water-excluded/lipid environments that do allow photoswitching, giving comparatively slow cell-averaged rates of spontaneous *E*-to-*Z* relaxation, yet with rapid exchange from the aprotic environment supplying the photopatterned isomer ratio to the cytosol.[31] We therefore reasoned that a sufficiently soluble pyrrole hemithioindigo photopharmaceutical might apply a cellular FDR approaching this high FDR_{max}, as its photostationary state equilibria (PSSs) could reflect those of apolar media.

This we determined to test experimentally, evaluating the PHT scaffold in the biological context through proof-of-concept applications photocontrolling the dynamics of the MT cytoskeleton. This led us to design **PHTub**s, PHT-based photopharmaceuticals intended to isomer-dependently bind tubulin at the colchicine site, for cellular use as photoswitchable antimitotics and cytoskeleton inhibitors aiming at high-FDR and high-spatiotemporal-resolution photocontrol of cell cycle, cell viability, and cellular MT dynamics.

Results

Design and Synthesis

We designed **PHTub**s as PHT-based close steric analogues of the MT inhibitor colchicine. The colchicine pharmacophore consists of two aryl blades: a "southern" di- or tri-methoxyaryl ring, fixed close to a "northern" ring projecting a methoxy or ethyl spacefilling group (Figure 1b).[32] We chose the thioindoxyl to replace the southern ring to permit flexible substitution, leaving the pyrrole ring to bear the single ethyl group. We created nine **PHTub**s to scan orientations of the di/trimethoxy and ethyl substituents seeking both potency and isomer-dependency of bioactivity.

Of these, we expected that the 3′-ethyl **PHTub-3/6/9** would not bind tubulin with high affinity in either isomer due to the misoriented projection of the ethyl group (Figure 1b). We therefore expected **PHTub-3/6/9** would serve as useful regioisomeric controls, mismatching the SAR understood for the desired biological target. We and others[33] use regioisomeric controls to test for nonspecific bioactivity: both the classic effects of pan-assay interference compounds (PAINS) that must be anticipated for hydrophobic photoswitches (e.g., promiscuous binding, aggregation on proteins, or membrane disruption);[34] as well as nonspecific scaffold toxicity or phototoxicity under illumination.[22] By excluding such activity, regioisomeric controls can support that other compounds designed to match the target SAR act isomer-dependently and target-specifically (see Supporting Note 1). We also synthesised an N-methylated control **PHTub-NMe** that we expected to be inactive due to a steric clash (of the N-methyl group with the binding pocket wall),[21] but we were interested to study the effects of suppressing the NH···O=C hydrogen bond upon its photochemistry and, potentially, bioactivity (Figure 1c).

These **PHTub**s were synthesised in four to eight steps, assembling the PHT cores by piperidine-catalysed aldol condensation of ethylpyrrole-2-carbaldehydes onto methoxylated thioindoxyls (Figure 1d, Scheme S2, see Supporting Information).

Photoswitching

The **PHTub**s could be photoswitched in dry or in 25% aqueous polar media, under air, over multiple cycles without degradation (Figure 2a, Figure S2–S5). We would expect these lipophilic **PHTub**s to concentrate in water-excluded environments in cells, and so to display good cellular photoswitchability at 430–450 nm (giving ca. 90% *E*) vs. 515–530 nm (giving ca. 95% *Z*; Figure 2b, Figure S8, Table S4). By low photoresponse to > 550 nm we also expected that they could permit orthogonal imaging in the red fluorescent protein (RFP) channel at 561 nm.

Matching expectations from Newhouse and Zweig,[27] the band separation of PHT isomers (and thus the FDR_{max}) depended on the solvent's capacity to interrupt the internal H-bond, with ca. 45 nm separation in aprotic dry MeCN (FDR_{max} ca. 20-fold at 440/525 nm for all compounds)

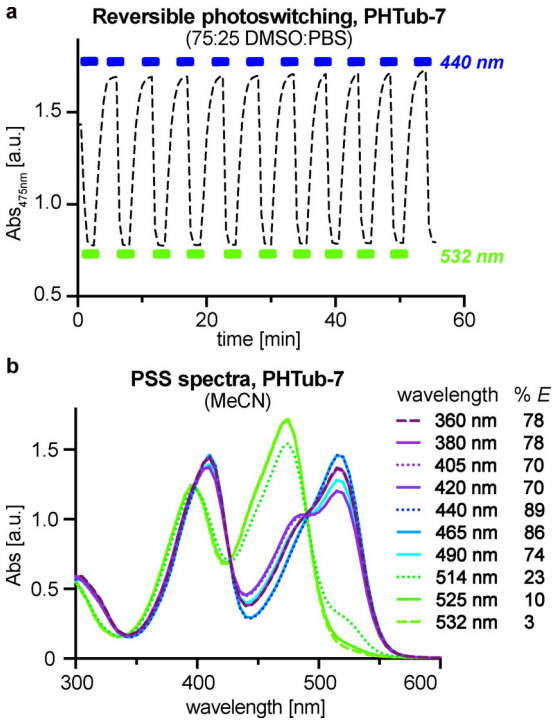

Figure 2. Photoswitching: a) **PHTub-7** is robustly and reversibly photoswitched from a majority-*Z* to a majority-*E* photostationary state (PSS) at 440 nm, and back to majority-*Z* with 532 nm. b) **PHTub-7** PSS absorbance spectra (UV/Vis spectroscopy) and composition (HPLC analysis) when illuminated with biocompatible wavelengths.

decreasing to ca. 30 nm in 75:25 DMSO:PBS (FDR_{max} below 10-fold, Table S2). N-methylated **PHTub-NMe** had similar photoswitching as phenyl hemithioindigo in both apolar solvents and DMSO:PBS, highlighting the role of the NH···O=C hydrogen bond in reaching high FDR. While the 3′/4′-ethylated PHTs had all-*Z* dark-adapted states, 5′-ethylated **PHTub-3/6/9** seemed to have nonzero *E* isomer proportion in the dark-adapted state (Figure S5 and discussion in the Supporting Information). Typical *E*-to-*Z* relaxation half-lives were in the hours to minutes range, being fastest in hydrogen-bond-disrupting polar solvents (Figure S6,7). **PHTub**s withstood challenge by 10 mM GSH over hours, and during repeated cycles of *Z*–*E* isomerization and thermal relaxation (Figure S9). This contrasts favourably to similarly polymethoxylated *Z*-azobenzenes that are destroyed by thiols.[21]

We therefore began exploring the applicability of PHT as an in situ-photoswitchable scaffold for cell biology through the use of **PHTub**s as photoswitchable MT inhibitors.

Structure-and-Photoisomer-Activity Relationship

Microtubule inhibition blocks cell proliferation, ultimately inducing cell death.[35] Therefore, we initially assessed the cellular bioactivity of the **PHTub**s by assaying their antiproliferative activity, in 44 hour assays in both HeLa cervical cancer and Jurkat T-cell leukaemia cell lines, under regularly pulsed illuminations designed to test both *E* and *Z* PHT isomers (Table 1).[3]

Table 1: IC_{50} values of all **PHTub**s in HeLa and Jurkat cell lines as *majority-*Z* and *majority-*E* isomer mixtures.[a]

	IC_{50} HeLa [μM]		IC_{50} Jurkat [μM]	
compound	*Z*-PHTub*	*E*-PHTub*	*Z*-PHTub*	*E*-PHTub*
PHTub-1	> 30 (n.sol.)	1.8	10	2
PHTub-2	0.2	0.4	0.1	0.3
PHTub-3	13	3.2	9	3.5
PHTub-4	> 100	ca. 9	4	ca. 20
PHTub-5	> 100	11	> 100	3
PHTub-6	> 20 (n.sol.)	ca. 20 (n.sol.)	> 20 (n.sol.)	> 20 (n.sol.)
PHTub-7	> 50 (n.sol.)	4.5	> 50 (n.sol.)	3.5
PHTub-8	0.07	0.12	0.03	0.05
PHTub-9	6.3	5.5	4.5	4.3
PHTub-NMe	> 20 (n.sol.)	ca. 20 (n.sol.)	> 20 (n.sol.)	ca. 20 (n.sol.)

[a] *Majority-*Z* by illumination at 525–535 nm or by dark conditions; *majority-*E* by illumination at 435–450 nm; 44 h incubation; illuminations pulsed at 75 ms per 15 s with < 3 mW cm^{-2}; three independent experiments; n.sol. indicates apparent bioactivity near the solubility limit, which we attribute to aggregation; see Supporting Information for details.

PHTub-4/5/6 gave low-potency effects that match expectations for weak, nonspecific toxicity of low-solubility compounds near their aggregation threshold. We interpret this as a lack of tubulin binding, due to a steric clash of their south ring's outer methoxy group with the T7 loop of the colchicine site.[20,22] Yet, as both di- and tri-methoxyaryl rings can be tolerated in the southern binding lobe,[32] we expected that deleting the outer methoxy (**PHTub-1/2/3**) or shifting it around the ring (**PHTub-7/8/9**) could permit cytotoxicity, and both were confirmed. In these series, the position of the northern ethyl group was the major determinant of both isomers' bioactivity, which corresponded between the sets (e.g. **PHTub-1** corresponding to **PHTub-7**).

4′-Ethyl **PHTub-2/8** achieved excellent potency: superior to all photoswitchable tubulin binders yet reported[3,21,31] and near to colchicine site binders used as drugs (**PHTub-8** IC_{50}s $\leq$ 120 nM, colchicine ca. 20 nM), although their bioactivity was only slightly photoswitchable (*Z*-**PHTub2/8** ca. 2× as potent as the *E* isomers).

Shifting to a 5′-ethyl group in **PHTub-1/7** sacrificed potency, but greatly improved the photoswitchability of bioactivity: a necessary compromise for effective photopharmaceuticals. *E*-**PHTub-1** had good potency (mostly-*E*-**PHTub-1** IC_{50} ca. 2 μM in Jurkat and HeLa), while *Z*-**PHTub-1** gave only weak irreproducible bioactivity above 10 μM, which we attributed to its aggregation rather than to tubulin binding. We have observed elsewhere that the out-of-plane middle methoxy group of a 3,4,5-trimethoxyphenyl motif brings significant solubility benefits compared to dimethoxyphenyl, which can suppress aggregation effects and so increase the photoswitchability of bioactivity.[3] We were delighted to see this in **PHTub-7**, which retained similarly good potency under blue illumination (mostly-*E*-**PHTub-7** IC_{50} ca. 3–5 μM in Jurkat and HeLa), yet gave no visible effects as the *Z* isomer at even 10–17-fold higher concentrations (< 10% antiproliferative effect up to 50 μM; Figure 3a,b).

Shifting instead to a 3′-ethyl group showed that **PHTub-1/7** are at a local optimum for the photoswitchability of bioactivity. **PHTub-3** was active (*E*-$IC_{50} = 3$ μM) but had only

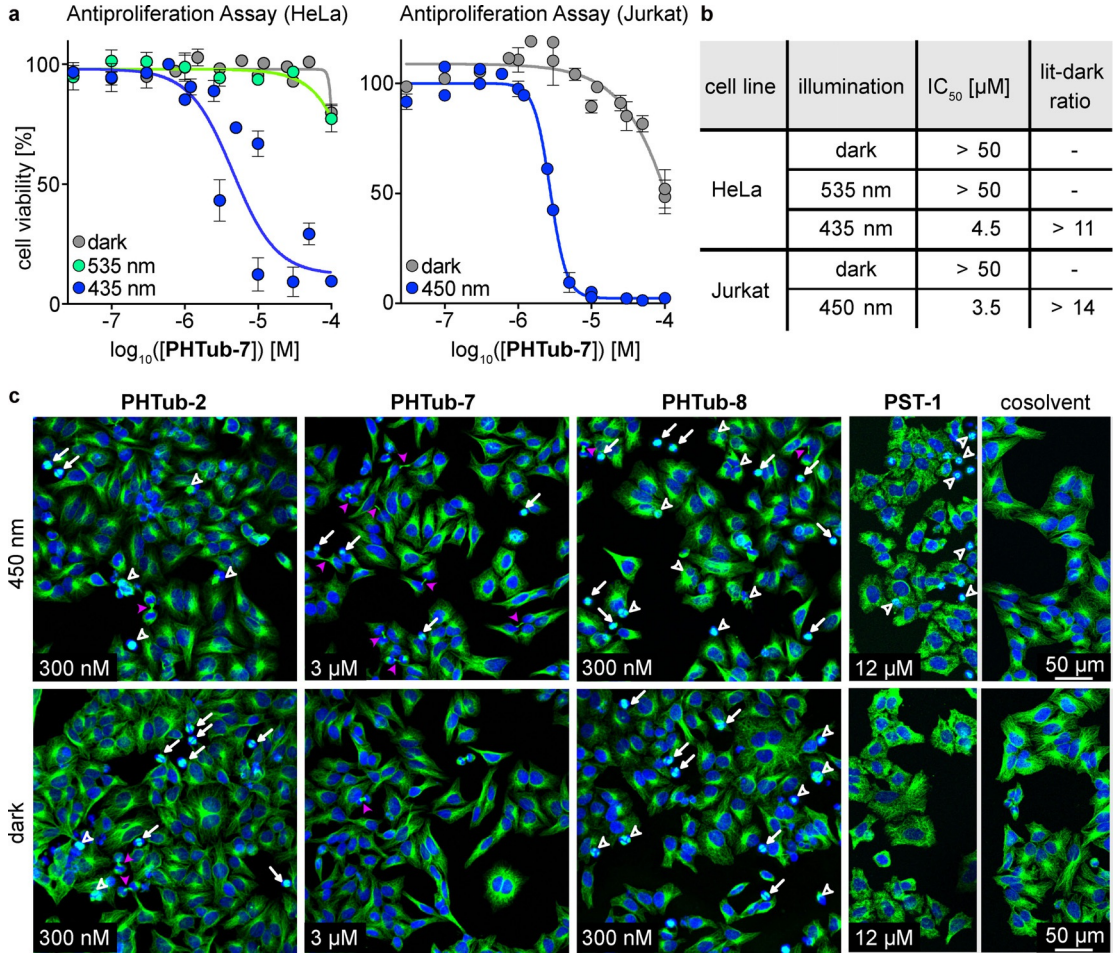

cell line	illumination	IC_{50} [µM]	lit-dark ratio
HeLa	dark	> 50	-
	535 nm	> 50	-
	435 nm	4.5	> 11
Jurkat	dark	> 50	-
	450 nm	3.5	> 14

Figure 3. **PHTub** bioactivity is light-specific and tubulin-mediated. a,b) **PHTub-7** gave strong light-specific antiproliferative effects with wavelength-dependency aligning to cell-free PSS measurements (HeLa and Jurkat cells; where for comparison, **PST-1** IC_{50}s: HeLa 1 µM (435 nm), 40 µM (dark); Jurkat 80 nM (435 nm), 20 µM (dark)). c) Immunofluorescence imaging of microtubule network architecture in HeLa cells treated with **PHTub-2**/**7**/**8** or cosolvent only, under pulsed 450 nm illumination or dark conditions. White arrows indicate mitotic arrests, hollow white arrowheads indicate multipolar spindles and other mitotic failures, filled pink arrowheads indicate remnant cytokinetic bridges (12 h incubation; α-tubulin in green, DNA stained with DAPI in blue).

mediocre photoswitchability of bioactivity (3-fold), while **PHTub-9** was similarly and not strongly active as both isomers. **PHTub-NMe**, whose *N*-methyl group similarly acts a spacefilling group adjacent to the double bond, was fully inactive as both isomers (Table 1).

Taken together, the ordered structure–activity relationships of the **PHTub**s (trimethoxy orientation and spacefill location) are consistent with those expected for colchicine site binders.[32] The demonstration of weakly potent light-independent regioisomer controls, for example, **PHTub-6**/**9**, and highly-potent but nearly-light-independently active **PHTub-2**/**8**, argues that phototoxicity or other nonspecific toxicities are not relevant for the **PHTub**s or the PHT scaffold. Due to its excellent photoswitchability of bioactivity, we proceeded into further biological testing with **PHTub-7** as our lead PHT photopharmaceutical. In parallel, we used **PHTub-2**/**8** interchangeably as low-photoswitchability but highly bioactive controls likely to share *E*-**PHTub-7**'s mechanism of action.

Tubulin-Specific Mechanism of Action in Cells

To test the tubulin-specificity of their light-dependent cytotoxicity, we first imaged the endogenous microtubule (MT) network architecture in cells incubated with **PHTub**s, to observe direct effects on their desired target protein. The nanomolar-potent **PHTub-2**/**8** caused a high proportion of mitotic arrests (arrows) and multipolar spindles or other mitotic failures (hollow arrowheads) under both illumination conditions (Figure 3c), reflecting expectations from their cytotoxicity assays. **PHTub-7** was less potent in its effects, matching the cytotoxicity results: but the 450 nm-specific accumulation of mitotic arrests and of abnormal remnant cytokinetic bridges (filled arrowheads)—a hallmark of perturbed mitosis[36]—was notable, whereas this was almost not seen in dark conditions (Figure 3c). Cell-free assays testing inhibition of the polymerisation of purified tubulin protein supported a direct tubulin-binding mechanism of action for the **PHTub**s, with **PHTub-7** and **PHTub-8** displaying comparable potency as the reference colchicine site inhibitors,

nocodazole and colchicine, yet with isomer-dependent bioactivity matching, respectively the lit-activity and dark-activity of the cellular assays (Figure S10). We concluded that **PHTub**s were supported as cellularly active inhibitors binding tubulin.

To crosscheck if the major cellular bioactivity mechanism of the **PHTub**s is MT inhibition, we examined their induction of light-dependent G_2/M-phase cell cycle arrest at their antiproliferative concentrations, which is a hallmark of microtubule inhibitors.[32] Using flow cytometric analysis we observed, as expected, induction of G_2/M arrest for *E*-**PHTub-7** but not for *Z*-**PHTub-7** (Figure 4), while **PHTub-2** gave potent but nearly light-independent cell cycle arrest (Figure S12). This further supports that *E*-**PHTub-7** potently inhibits MT function while *Z*-**PHTub-7** does not, suiting it to photoswitching-based control of MT-dependent processes.

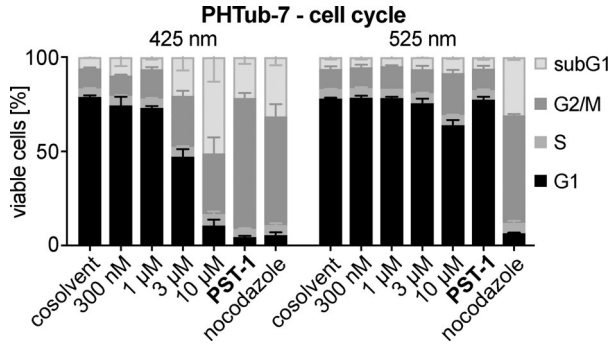

Figure 4. Cell cycle photocontrol. Cells treated with **PHTub-7** under 425 nm pulsing show significant G2/M arrest and cell death (sub-G1 phase cells), similar to that seen with reference MT inhibitor **PST-1** (12 µM) and light-independently with nocodazole (300 nM); but **PHTub-7** has no effects under 525 nm pulsing (compare to DMSO cosolvent-only controls).

Live Cell Photocontrol of Microtubule Dynamics by In Situ PHTub Photoswitching

We next tested the suitability of **PHTub**s (and by extension, the PHT scaffold) for spatially and temporally precise live cell photoswitching uses in confocal microscopy. This is a significant advance for photopharmacology, since as far as we know, no hemithioindigo derivatives have yet been demonstrated in temporally resolved live cell studies with spatially resolved in situ photoswitching. To do so, we imaged microtubule dynamics in HeLa cells transfected with fluorescently labelled end binding proteins (EBs). EBs mark the GTP cap regions of polymerising MTs. Thus, imaging EBs reveals the plus ends of polymerising MTs as dynamic comets;[37] and imaging during photoswitching is a spatiotemporally resolved readout for isomerisation-dependent inhibition of MT dynamics by photoswitchable inhibitors.[3,38]

We first confirmed that *Z*-**PHTub-7** (dark state) has no significant residual effects on MT dynamics by imaging tdTomato-EB3 at 561 nm; *Z*-**PHTub-7** caused no significant change of MT dynamics compared to DMSO controls (Figure 5).

Next, we applied 442 nm laser pulses to photoisomerise **PHTub-7** in situ to the *E* isomer throughout the field of view. This drastically suppressed cellular MT dynamics with high temporal precision (Figure 5a,b). MT dynamics did not recover over minutes; in light of further experiments, we believe this indicates that *E*-**PHTub-7** does not rapidly diffuse out of cells because it is lipophilic (intracellular "sinks";[39] see below).

442 nm is nearly an ideal photoactivation wavelength for PHTs (Table S4), but it is not a very common laser line on the confocal microscopes where MT research is performed. However, GFP-exciting lasers (typically 487, 488, or 491 nm) are standard on all confocal microscopes. We therefore tested whether GFP lasers are suitable for cellular photoactivation of **PHTub-7**. Indeed, 487 nm illumination also caused reproducible inhibition of MT dynamics (Figure 5c,d; Movie S1), although with slower response than 442 nm. These useful results show that PHT-based photopharmaceuticals can be photoisomerised using standard blue or cyan confocal microscope lasers, that have low potential for phototoxicity in cell research (see also Supporting Note 2). This contrasts favourably to most photocages and to most other photopharmaceuticals that require UV (355 nm laser) or near-UV (405 nm laser) photoactivations.

To crosscheck the mechanism of action of **PHTub-7**, we also imaged its potent congener **PHTub-8**, which had appeared more active as its dark (*Z*) isomer than in its lit state. Encouragingly, we observed both that *Z*-**PHTub-8** suppresses MT dynamics and that in situ 442 or 487 nm illumination caused drastic acceleration of MT polymerisation for a short while. Photoaccelerations could typically be performed at least three times before their magnitude became less impressive (Figure 5e,f; Movie S3; see Discussion). These results match the dark-activity of its cytotoxicity and immunofluorescence assays, so supporting that both **PHTub7/8** directly and photoswitchably inhibit tubulin.

Lastly, we performed cell-precise photoisomerisations of **PHTub-7** in single selected cells, hoping to temporally precisely block MT dynamics in those cells, without affecting their neighbour cells. In cells targeted with 442 nm laser regions (ROIs), EB3 comet counts dropped even below what had been seen with full field of view photoactivations, and did not recover over minutes, while neighbour cells remained unaffected as in non-treated and non-illuminated cosolvent controls (Figure 5g,h; Movie S4). By excluding bulk photoisomerisation in the medium, this supports the idea of intracellular sinks[39] of slowly diffusing **PHTub** being responsible for cell-persistent effects. (It also contrasts to diffusional recovery (approx. 30 s) observed for other scaffolds, such as the styrylbenzothiazole *Z*-**SBTub3**[21]).

Thus, **PHTub-7** can inhibit MT dynamics of target cells with temporal precision on the scale of seconds and spatial precision on the single-cell level. Taken together, these experiments also demonstrate that the PHT scaffold may more generally be uniquely suited for in situ photoswitching use in live cells with standard confocal microscope lasers, as part of both dark- or lit-active photopharmaceuticals, also against other protein targets.

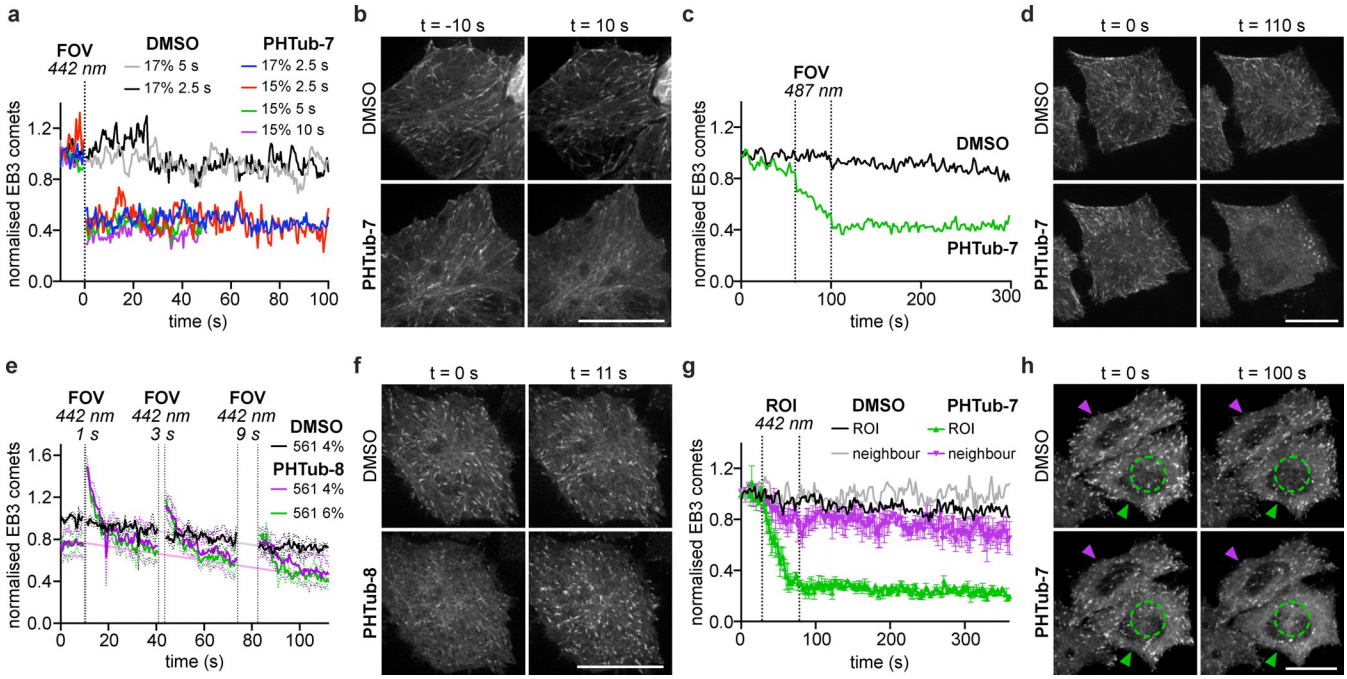

Figure 5. **PHTub**s enable in situ photoswitching of MT dynamics in live cells. a–d) MT dynamics are temporally precisely suppressed when cells treated with lit-active ***Z*-PHTub-7** (2 μM) are illuminated within the field of view (FOV) at a,b) 442 nm or at c,d) 487 nm (related to Movie S1). e,f) Cells treated with dark-active ***Z*-PHTub-8** (0.5 μM) have suppressed MT dynamics, which can be repeatedly accelerated by illuminations at 442 nm (related to Movie S3). Photobleaching background rate fits (grey: DMSO, pink: treated) are guides to the eye to distinguish accelerations. g,h) Cell-precise MT dynamics suppression is caused by 442 nm photoactivation of ***Z*-PHTub-7** (2 μM) within a subcellular region of interest (shown by green circle) in a target "ROI" cell (green arrowhead), while adjacent "neighbour" cells without photoactivation (pink arrowhead) do not show altered MT dynamics (related to Movie S4; EB3-tdTomato-transfected HeLa cells; tdTomato imaged at 561 nm; normalised EB3 "comet" counts quantify dynamic MTs; b/d/f/h: scale bars indicate 20 μm; for full caption and details see Supporting Information).

Discussion

Photopharmacological approaches to high-spatiotemporal-precision manipulation of endogenous proteins have progressed significantly, enabling biological application to membranes, ion channels, and the cytoskeleton.[1,9,40] Photopharmaceuticals for the cytoskeleton have transitioned rapidly beyond their cellular proofs of concept showing non-invasive, reversible, cellularly resolved optical control over MT dynamics and network structure.[41] For example, despite the relatively poor functional dynamic range of the azobenzene **PST**s (3-fold at 405/514 nm), they have found high-precision uses in embryonic fruit fly *D. melanogaster*,[42] worm *C. elegans*,[3] zebrafish *D. rerio*,[43] and mouse *M. musculus*,[44] where they have helped to resolve questions in development and in neuroscience.[45,46] Such uses illustrate the power of photopharmacology to enable previously inaccessible studies of spatiotemporally complex processes.

However, the scope of photopharmacology remains restricted by the photochemical and biochemical limitations of its photoswitch scaffold repertoire.[47] Several limitations of the major scaffold azobenzene, including the diazene's susceptibility to thiol-mediated degradation and its restricted scope of substituents compatible with bistable photoswitch performance, are well-known.[21] Non-azobenzene photoswitches that avoid these drawbacks, such as dithienylethenes, hemithioindigos, and heterostilbenes, have only recently begun to be used in bioactive pharmacophores validated in cellular studies;[21,22,48] and the development of new photoswitch scaffolds is a valuable research goal in general.[49] Yet, while some recently developed scaffolds have approached near-quantitative bidirectional photoswitching in physiological media,[50] there is still no clear choice of scaffold that can robustly ensure this performance in cells using the light sources that are actually available in biological research.

Here we show that PHT may be a general photopharmaceutical alternative to azobenzenes, offering comparable size and chemical simplicity, but better GSH resistance, more cell-compatible photoisomerisation wavelengths, and a better match of its optimum photoisomerisation wavelengths to those available on all confocal microscopes.

We had particularly sought to develop a photopharmaceutical with a high functional dynamic range (FDR). Towards this end, we hoped that with the **PHTub**s' hydrophobicity favouring biolocalisation in water-excluded environments, their cellular photoswitching could approach the excellent PSSs that PHT shows in organic media.[27] This is not yet generally recognised as a design opportunity for photopharmacology, but we believe it is an important one. Tuning photochemistry dependent on cellular/local environment has long been exploited in fluorescence microscopy[51] and its applications are advancing rapidly;[52] and environment-dependency has been observed experimentally for photoswitches (e.g. hypsochromic shifts of optimum *E*-to-*Z* isomer-

isation wavelength in membranes;[53] 60 nm bathochromic shifts upon protein binding[54]). The photoswitchability of bioactivity observed with **PHTub-7** in this work suggests that PHT's favourable organic-media photochemistry can indeed be harnessed for cellular applications. This suggests new design opportunities for photopharmaceuticals to bring high functional dynamic range photoswitching to bear in biology.

Additionally, through **PHTub-8**, we have given the first demonstration of time-resolved live cell photocontrol of a dark-active cytoskeleton photopharmaceutical. Though its reversibility was limited, this achievement is conceptually significant: because reversible dark-active photocontrol over biological processes using stoichiometric inhibitors is more challenging to achieve than with highly nonlinearly acting modulators (as have been used to control, for example, excitable cell firing[55]). Reversible stoichiometric control requires (i) high in situ photoconversion to the less bioactive metastable isomer (i.e. high practical FDR), which is typically problematic for photoswitch scaffolds (other than PHTs); and (ii) high isomer specificity of bioactivity, which is typically problematic for their bioactive derivatives (other than some colchicinoids). Although *E*-**PHTub-8** had significant residual bioactivity, its high FDR—achieved by matching the PHT scaffold's peak isomerisation efficiency to the GFP laser—was crucial for its success in achieving photoaccelerations. We also believe that enhanced dark-active compounds based on **PHTub-8** can be useful tools for localised induction of MT polymerisation in biology, which remains a high-value goal of reagent development.[40,56]

It was interesting that **PHTub-8** appeared somewhat reversible while **PHTub-7** did not (Figure 5e,g). We discount three suggestions for reversibility that are usually significant for photopharmacology (diffusion into/out of cells; spontaneous *E*-to-*Z* relaxation; and *E*-to-*Z* photoreversion of **PHTub8** by 561 nm imaging) due to the results of control experiments (see Supporting Note 3). We propose instead that **PHTub-8** reversibility arises since upon each 442/487 nm photoisomerisation, partial *E*-**PHTub-8** unbinding from tubulin monomers "injects" tubulin into the polymerisable pool, so polymerisation rate and comet count transiently increase. This excess is then "used up" by addition to MT polymer; and over ca. 10 s the cell returns to steady state MT dynamics. Thus at each subsequent 442/487 nm photoisomerisation pulse, there is less tubulin monomer that can be injected, and rate enhancements become smaller. These considerations can have general interest for photopharmacology.

Conclusion

In this work we have applied the pyrrole hemithioindigo (PHT) photoswitch scaffold to develop a rationally designed series of photopharmaceutical reagents for in situ-photoswitching-based optical control over the cellular microtubule (MT) cytoskeleton: a critical biological target in urgent need of reagents enabling high-resolution modulation assays.[41] The choice of the PHT scaffold was driven by its superior photoswitching performance at microscopy laser lines. We have demonstrated these **PHTub** reagents' capacity to apply optical control over MT network integrity, cell division, and cell death in long-term assays. In short-term assays, they achieve temporally resolved, cell-specific, optical modulation of MT dynamics in live cells. To our knowledge this is the first high-resolution live cell application of any hemithioindigo as a photopharmaceutical pharmacophore; and its success highlights both the **PHTub**s' and the PHT scaffold's promise for a range of high-spatiotemporal-precision biological studies. We therefore believe that **PHTub-7** in particular will be a valuable photopharmaceutical for high-precision cytoskeleton research, with promising applications in the fields of cellular transport, mechanostasis, migration, cell division, and embryonic development.

This research also suggests that the PHT scaffold too will find a broad range of applications to biological targets that are poorly addressed by current photopharmaceuticals. These targets may be located both cytosolically, as well as in water-excluded environments where the PHT scaffold may be even more advantageously applicable. Novel photoswitches that can be introduced into known photopharmaceutical designs to retain their on-target bioactivity while accessing new photochemical performance are rightly recognised as high-value targets in photopharmacology (e.g. spectrally shifted diazocines,[57,58] tetra-*ortho*-substituted azobenzenes,[15,59] and azoniums[60]). Therefore it is broadly significant that the similar molecular design of **PHTub-7** compared to its azobenzene analogues (**PST**s) ensured similar isomer-dependent bioactivity. Our work thus suggests that Zweig and Newhouse's pyrrole hemithioindigos[27] may be generally useful as a straightforward alternative to azobenzenes in photopharmacology, for powerful photopharmaceuticals with higher functional dynamic ranges under standard microscopy lasers, useful against a range of biological targets.

Acknowledgements

We are grateful to Henrietta Lacks, now deceased, and to her surviving family members for their contributions to biomedical research. We thank E. Fajardo-Ruiz (LMU) for tubulin polymerisation assays; D. Lonken (LMU) for early PHTub viability testing; and Marie Delattre (ENS Lyon, FR) and Wallis Nahaboo (University of Brussels, BE) for early development of cellular photoswitchability of hemithioindigos. We thank Peter Mayer (LMU) for X-ray data and Werner Spahl (LMU) for mass spectra. Deposition Number 2089743 contains the supplementary crystallographic data for this paper. These data are provided free of charge by the joint Cambridge Crystallographic Data Centre and Fachinformationszentrum Karlsruhe Access Structures service www.ccdc.cam.ac.uk/structures. J.T.-S. thanks the Joachim Herz foundation for grant support. O.T.-S. thanks the German Research Foundation (DFG: Emmy Noether grant number 400324123, SFB 1032 project B09 number 201269156, SFB TRR 152 project P24 number 239283807, SPP 1926 project XVIII number 426018126) and the Munich Centre for NanoScience initiative (CeNS) for funding. J.C.M.M. acknowledges sup-

port from an EMBO Long Term Fellowship. Open Access funding enabled and organized by Projekt DEAL.

Conflict of Interest

The authors declare no conflict of interest.

Keywords: cytotoxicity · hemithioindigo · microtubule dynamics · photopharmacology · photoswitch

[1] A. Rullo, A. Reiner, A. Reiter, D. Trauner, E. Y. Isacoff, G. A. Woolley, *Chem. Commun.* **2014**, *50*, 14613 – 14615.
[2] L. Agnetta, M. Kauk, M. C. A. Canizal, R. Messerer, U. Holzgrabe, C. Hoffmann, M. Decker, *Angew. Chem. Int. Ed.* **2017**, *56*, 7282 – 7287; *Angew. Chem.* **2017**, *129*, 7388 – 7393.
[3] M. Borowiak, W. Nahaboo, M. Reynders, K. Nekolla, P. Jalinot, J. Hasserodt, M. Rehberg, M. Delattre, S. Zahler, A. Vollmar, D. Trauner, O. Thorn-Seshold, *Cell* **2015**, *162*, 403 – 411.
[4] J. Joshi, M. Rubart, W. Zhu, *Front. Bioeng. Biotechnol.* **2020**, *7*, 466.
[5] R. Weinstain, T. Slanina, D. Kand, P. Klán, *Chem. Rev.* **2020**, *120*, 13135 – 13272.
[6] M. J. Fuchter, *J. Med. Chem.* **2020**, *63*, 11436 – 11447.
[7] P. Klán, T. Šolomek, C. G. Bochet, A. Blanc, R. Givens, M. Rubina, V. Popik, A. Kostikov, J. Wirz, *Chem. Rev.* **2013**, *113*, 119 – 191.
[8] K. Hüll, J. Morstein, D. Trauner, *Chem. Rev.* **2018**, *118*, 10710 – 10747.
[9] M. Borowiak, F. Küllmer, F. Gegenfurtner, S. Peil, V. Nasufovic, S. Zahler, O. Thorn-Seshold, D. Trauner, H.-D. Arndt, *J. Am. Chem. Soc.* **2020**, *142*, 9240 – 9249.
[10] B. T. Castle, D. J. Odde, *Cell* **2015**, *162*, 243 – 245.
[11] T. Wittmann, A. Dema, J. van Haren, *Curr. Opin. Cell Biol.* **2020**, *66*, 1 – 10.
[12] S. Florian, T. J. Mitchison in *The Mitotic Spindle: Methods and Protocols* (Eds.: P. Chang, R. Ohi), Springer New York, New York, **2016**, pp. 403 – 421.
[13] J. R. Peterson, T. J. Mitchison, *Chem. Biol.* **2002**, *9*, 1275 – 1285.
[14] M. J. Fuchter, *J. Med. Chem.* **2020**, *63*, 11436—11447.
[15] D. B. Konrad, G. Savasci, L. Allmendinger, D. Trauner, C. Ochsenfeld, A. M. Ali, *J. Am. Chem. Soc.* **2020**, *142*, 6538—6547.
[16] C. E. Weston, R. D. Richardson, P. R. Haycock, A. J. P. White, M. J. Fuchter, *J. Am. Chem. Soc.* **2014**, *136*, 11878 – 11881.
[17] A. J. Engdahl, E. A. Torres, S. E. Lock, T. B. Engdahl, P. S. Mertz, C. N. Streu, *Org. Lett.* **2015**, *17*, 4546 – 4549.
[18] J. E. Sheldon, M. M. Dcona, C. E. Lyons, J. C. Hackett, M. C. T. Hartman, *Org. Biomol. Chem.* **2016**, *14*, 40 – 49.
[19] S. K. Rastogi, Z. Zhao, S. L. Barrett, S. D. Shelton, M. Zafferani, H. E. Anderson, M. O. Blumenthal, L. R. Jones, L. Wang, X. Li, C. N. Streu, L. Du, W. J. Brittain, *Eur. J. Med. Chem.* **2018**, *143*, 1 – 7.
[20] R. Gaspari, A. E. Prota, K. Bargsten, A. Cavalli, M. O. Steinmetz, *Chem* **2017**, *2*, 102 – 113.
[21] L. Gao, J. C. M. Meiring, Y. Kraus, M. Wranik, T. Weinert, S. D. Pritzl, R. Bingham, E. Ntouliou, K. I. Jansen, N. Olieric, J. Standfuss, L. C. Kapitein, T. Lohmüller, J. Ahlfeld, A. Akhmanova, M. O. Steinmetz, O. Thorn-Seshold, *Cell Chem. Biol.* **2021**, *28*, 228 – 241.
[22] A. Sailer, F. Ermer, Y. Kraus, F. Lutter, C. Donau, M. Bremerich, J. Ahlfeld, O. Thorn-Seshold, *ChemBioChem* **2019**, *20*, 1305 – 1314.
[23] N. Regner, T. T. Herzog, K. Haiser, C. Hoppmann, M. Beyermann, J. Sauermann, M. Engelhard, T. Cordes, K. Rück-Braun, W. Zinth, *J. Phys. Chem. B* **2012**, *116*, 4181 – 4191.
[24] S. Kitzig, M. Thilemann, T. Cordes, K. Rück-Braun, *ChemPhysChem* **2016**, *17*, 1252 – 1263.
[25] F. Kink, M. P. Collado, S. Wiedbrauk, P. Mayer, H. Dube, *Chem. Eur. J.* **2017**, *23*, 6237 – 6243.
[26] K. Stallhofer, M. Nuber, F. Schüppel, S. Thumser, H. Iglev, R. de Vivie-Riedle, W. Zinth, H. Dube, *J. Phys. Chem. A* **2021**, *125*, 4390 – 4400.
[27] J. E. Zweig, T. R. Newhouse, *J. Am. Chem. Soc.* **2017**, *139*, 10956 – 10959.
[28] J. Gavin, J. F. M. Ruiz, K. Kedziora, H. Windle, D. P. Kelleher, J. F. Gilmer, *Bioorg. Med. Chem. Lett.* **2012**, *22*, 7647 – 7652.
[29] D. M. Nikolaev, M. S. Panov, A. A. Shtyrov, V. M. Boitsov, S. Yu. Vyazmin, O. B. Chakchir, I. P. Yakovlev, M. N. Ryazantsev in *Progress in Photon Science: Recent Advances* (Eds.: K. Yamanouchi, S. Tunik, V. Makarov), Springer International Publishing, Cham, **2019**, pp. 139 – 172.
[30] J. E. Zweig, T. A. Ko, J. Huang, T. R. Newhouse, *Tetrahedron* **2019**, *75*, 130466.
[31] A. Sailer, F. Ermer, Y. Kraus, R. Bingham, F. H. Lutter, J. Ahlfeld, O. Thorn-Seshold, *Beilstein J. Org. Chem.* **2020**, *16*, 125 – 134.
[32] G. C. Tron, T. Pirali, G. Sorba, F. Pagliai, S. Busacca, A. A. Genazzani, *J. Med. Chem.* **2006**, *49*, 3033 – 3044.
[33] J. Lee, M. Schapira, *ACS Chem. Biol.* **2021**, *16*, 579 – 585.
[34] J. B. Baell, J. W. M. Nissink, *ACS Chem. Biol.* **2018**, *13*, 36 – 44.
[35] M. A. Jordan, K. Wendell, S. Gardiner, W. B. Derry, H. Copp, L. Wilson, *Cancer Res.* **1996**, *56*, 816 – 825.
[36] G. Normand, R. W. King in *Polyploidization and Cancer* (Ed.: R. Y. C. Poon), Springer New York, New York, **2010**, pp. 27 – 55.
[37] J. Roostalu, C. Thomas, N. I. Cade, S. Kunzelmann, I. A. Taylor, T. Surrey, *eLife* **2020**, *9*, e51992.
[38] A. Müller-Deku, J. C. M. Meiring, K. Loy, Y. Kraus, C. Heise, R. Bingham, K. I. Jansen, X. Qu, F. Bartolini, L. C. Kapitein, A. Akhmanova, J. Ahlfeld, D. Trauner, O. Thorn-Seshold, *Nat. Commun.* **2020**, *11*, 4640.
[39] K. Scherer, R. Bisby, S. Botchway, J. Hadfield, A. Parker, *J. Biomed. Opt.* **2014**, *20*, 051004.
[40] S. D. Pritzl, P. Urban, A. Prasselsperger, D. B. Konrad, J. A. Frank, D. Trauner, T. Lohmüller, *Langmuir* **2020**, *36*, 13509—13515.
[41] O. Thorn-Seshold, J. Meiring, *ChemRxiv* **2021**, https://doi.org/10.26434/chemrxiv.14424176.v1.
[42] A. Singh, T. Saha, I. Begemann, A. Ricker, H. Nüsse, O. Thorn-Seshold, J. Klingauf, M. Galic, M. Matis, *Nat. Cell Biol.* **2018**, *20*, 1126 – 1133.
[43] C. Vandestadt, G. C. Vanwalleghem, H. A. Castillo, M. Li, K. Schulze, M. Khabooshan, E. Don, M.-L. Anko, E. K. Scott, J. Kaslin, *bioRxiv* **2019**, 539940.
[44] J. Zenker, M. D. White, R. M. Templin, R. G. Parton, O. Thorn-Seshold, S. Bissiere, N. Plachta, *Science* **2017**, *357*, 925 – 928.
[45] J. Zenker, M. D. White, M. Gasnier, Y. D. Alvarez, H. Y. G. Lim, S. Bissiere, M. Biro, N. Plachta, *Cell* **2018**, *173*, 776 – 791.
[46] K. Eguchi, Z. Taoufiq, O. Thorn-Seshold, D. Trauner, M. Hasegawa, T. Takahashi, *J. Neurosci.* **2017**, *37*, 6043 – 6052.
[47] V. A. Gutzeit, A. Acosta-Ruiz, H. Munguba, S. Häfner, A. Landra-Willm, B. Mathes, J. Mony, D. Yarotski, K. Börjesson, C. Liston, G. Sandoz, J. Levitz, J. Broichhagen, *Cell Chem. Biol.* **2021**, https://doi.org/10.1016/j.chembiol.2021.02.020.
[48] N. A. Simeth, A. C. Kneuttinger, R. Sterner, B. König, *Chem. Sci.* **2017**, *8*, 6474 – 6483.
[49] M. W. H. Hoorens, M. Medved“, A. D. Laurent, M. Di Donato, S. Fanetti, L. Slappendel, M. Hilbers, B. L. Feringa, W. Jan Buma, W. Szymanski, *Nat. Commun.* **2019**, *10*, 2390.
[50] M. P. O'Hagan, J. Ramos-Soriano, S. Haldar, S. Sheikh, J. C. Morales, A. J. Mulholland, M. C. Galan, *Chem. Commun.* **2020**, *56*, 5186 – 5189.

[51] J. Kapuscinski, *Biotechnic & Histochemistry* **1995**, *70*, 220 – 233; Histochemistry **1995**, 70, 220 – 233.
[52] L. Wang, J. Hiblot, C. Popp, L. Xue, K. Johnsson, *Angew. Chem. Int. Ed.* **2020**, *59*, 21880 – 21884; *Angew. Chem.* **2020**, *132*, 22064 – 22068.
[53] P. Urban, S. D. Pritzl, D. B. Konrad, J. A. Frank, C. Pernpeintner, C. R. Roeske, D. Trauner, T. Lohmüller, *Langmuir* **2018**, *34*, 13368 – 13374.
[54] D. M. Barber, S.-A. Liu, K. Gottschling, M. Sumser, M. Hollmann, D. Trauner, *Chem. Sci.* **2017**, *8*, 611 – 615.
[55] P. Stawski, M. Sumser, D. Trauner, *Angew. Chem. Int. Ed.* **2012**, *51*, 5748 – 5751; *Angew. Chem.* **2012**, *124*, 5847 – 5850.
[56] K. B. Buck, J. Q. Zheng, *J. Neurosci.* **2002**, *22*, 9358 – 9367.
[57] M. S. Maier, K. Hüll, M. Reynders, B. S. Matsuura, P. Leippe, T. Ko, L. Schäffer, D. Trauner, *J. Am. Chem. Soc.* **2019**, *141*, 17295 – 17304.
[58] R. Siewertsen, H. Neumann, B. Buchheim-Stehn, R. Herges, C. Näther, F. Renth, F. Temps, *J. Am. Chem. Soc.* **2009**, *131*, 15594 – 15595.
[59] D. Bléger, J. Schwarz, A. M. Brouwer, S. Hecht, *J. Am. Chem. Soc.* **2012**, *134*, 20597 – 20600.
[60] S. Samanta, A. Babalhavaeji, M. Dong, G. A. Woolley, *Angew. Chem. Int. Ed.* **2013**, *52*, 14127 – 14130; *Angew. Chem.* **2013**, *125*, 14377 – 14380.

Manuscript received: April 7, 2021
Revised manuscript received: July 23, 2021
Accepted manuscript online: August 30, 2021
Version of record online: October 1, 2021

